

Timing and style of Late Quaternary glaciation in northeastern Tibet

Lewis A. Owen[†]

Department of Earth Sciences, University of California, Riverside, California 92521, USA

Robert C. Finkel

Center for Accelerator Mass Spectrometry, Lawrence Livermore National Laboratory, Livermore, California 94550, USA, and Department of Earth Science, University of California, Riverside, California 92521, USA

Ma Haizhou

Institute of Saline Lakes, Chinese Academy of Sciences, 18 Xining Road, Xining 810008, Qinghai, People's Republic of China

Joel Q. Spencer

School of Geography and Geosciences, University of Saint Andrews, Saint Andrews, Fife, KY16 9AL, Scotland, UK

Edward Derbyshire

Centre for Quaternary Research, Department of Geography, Royal Holloway, University of London, Egham, Surrey, TW20 0EX, UK

Patrick L. Barnard

Department of Earth Sciences, University of California, Riverside, California 92521, USA; and Center for Accelerator Mass Spectrometry, Lawrence Livermore National Laboratory, Livermore, California 94550, USA

Marc W. Caffee

Department of Physics/Purdue Rare Isotope Measurement Laboratory, Purdue University, West Lafayette, Indiana 47907, USA

ABSTRACT

Glacial successions in the Anyemaqen and Nianbaoyeze Mountains of northeastern Tibet are reassessed and new glacial chronologies are presented for these regions. Cosmogenic radionuclide and optically stimulated luminescence dating indicates that two glacial advances occurred in marine isotope stage (MIS)-3 and MIS-2. In the Anyemaqen Mountains, a third advance occurred in the Early Holocene. We suggest that glaciation was synchronous in the Anyemaqen and Nianbaoyeze Mountains, as well as in other glaciated areas of Tibet and the Himalaya that are influenced by the Asian monsoon. The maximum extent of glaciation occurred early in the last glacial cycle (MIS-3) during a time of increased insolation when the monsoon intensified and supplied abundant precipitation, as snow at high altitude, to feed high-altitude glaciers. This suggests that precipitation, as snow, is fundamental in controlling glaciation in these regions. However, the occurrence of glacial advances during the insolation min-

imum of MIS-2 suggests that, despite reduced precipitation at this time, the annual temperatures were cold enough to maintain positive glacier mass balances. The numerically defined chronologies for the Anyemaqen and Nianbaoyeze Mountains presented here provide a framework for comparing glacial advances in other parts of high Asia.

Keywords: Tibet, glaciation, monsoon, cosmogenic radionuclide dating, optically stimulated luminescence dating.

INTRODUCTION

The Tibetan Plateau is a feature of planetary scale that exerts a profound influence on regional and global atmospheric circulation. The interplay of atmospheric forces at work over the plateau and their relationship both to uplift and the broad climate swings that have characterized the Pleistocene and Holocene are therefore important for understanding the dynamics of global environmental change (Rudiman and Kutzbach, 1989; Molnar and England, 1990; Prell and Kutzbach, 1992; Owen et al., 2002d). One of the most direct effects

of the elevation and aridity of the Tibetan Plateau is the atmospheric warming it induces in spring and summer. The resulting low pressure over Tibet and South Asia is an important driver of the Asian monsoon, a system that dominates the regional climate of South Asia. The Asian monsoon supplies precipitation to the glacial and hydrological systems that ultimately provide water for hundreds of millions of people in central Asia. Long-term variability (thousands of years) of the Asian monsoon has been linked to external forcing through changes in Northern Hemisphere insolation, while shorter term variability (years to decades) has been related to internal changes of climate system variables such as Eurasian snow cover, the El Niño–Southern Oscillation, and tropical sea-surface temperatures (Hahn and Shukla, 1976; Dey and Bhanu Kumar, 1982; Dey et al., 1985; Dickson, 1984; Sirocko et al., 1991; Prell and Kutzbach, 1992; Soman and Slingo, 1997; Bush, 2000 and 2002). Furthermore, model results suggest that anthropogenic forcing (e.g., greenhouse gas and land cover change) has now become important in causing variations in the Asian monsoon (Wake et al., 2001).

Geologic landforms of Quaternary age on

[†]E-mail: lewis.owen@ucr.edu.

the Tibetan Plateau record evidence that is important for reconstructing changes in the regional climate and hydrology. However, the extent and timing of glaciation and the associated hydrological and climatic forcings and responses are poorly defined. This is partially because of the inaccessibility of the region but also because of the misinterpretation of glacial and non-glacial landforms and the lack of numerical dating to define the ages of landforms to establish regional correlations. Where studies have been undertaken, there has been little attempt to test the chronologies and reconstructions or to apply new methodologies and newly developing dating techniques.

To fill these gaps, we undertook a systematic study of two massifs in northeastern Tibet, the Anyemaqen and Nianbaoyeze Mountains (Fig. 1), to examine previous reconstructions of former glacier extent and to apply cosmogenic radionuclide (CRN) and optically stimulated luminescence (OSL) methods to date glacial landforms. The resulting glacial chronologies have allowed us to examine the relationship between glaciation and climate change.

GEOLOGIC SETTING

The Anyemaqen and Nianbaoyeze Mountains are situated in northeastern Tibet, trending northwest and lying ~100 km apart on either side of the Yellow River (Fig. 1A, inset). The Anyemaqen Mountains reach a maximum altitude of 6282 m above sea level (a.s.l.), rising from the surrounding peneplain at >4000 m a.s.l., and formed within a zone of transpression at the easternmost end of the Kunlun fault system (Van der Woerd et al., 2002). This range contains 40 glaciers and an ice cap with an area of ~120 km² that is the source of a few small outlet valley glaciers. The Nianbaoyeze Mountains rise from the surrounding plateau surface at a height of >4000 m a.s.l. to peaks that exceed 5000 m a.s.l. The main peak, at 5369 m a.s.l., comprises a granite dome that covers an area of ~820 km² (Lehmkuhl and Lui, 1994). The only contemporary glacier caps the highest peak and covers an area of ~5.1 km².

In both ranges the climate is dominated by the east Asian and south Asian monsoons in conjunction with low pressure and inward-blowing winds in summer (Wang, 1987; Lehmkuhl and Lui, 1994). Most of the precipitation falls in the summer months (~80% between May and October). Two precipitation peaks can be recognized; the first is caused by the East Asian monsoon and the second by the South Asian monsoon (Lehmkuhl and Lui, 1994). The total precipitation in the valleys

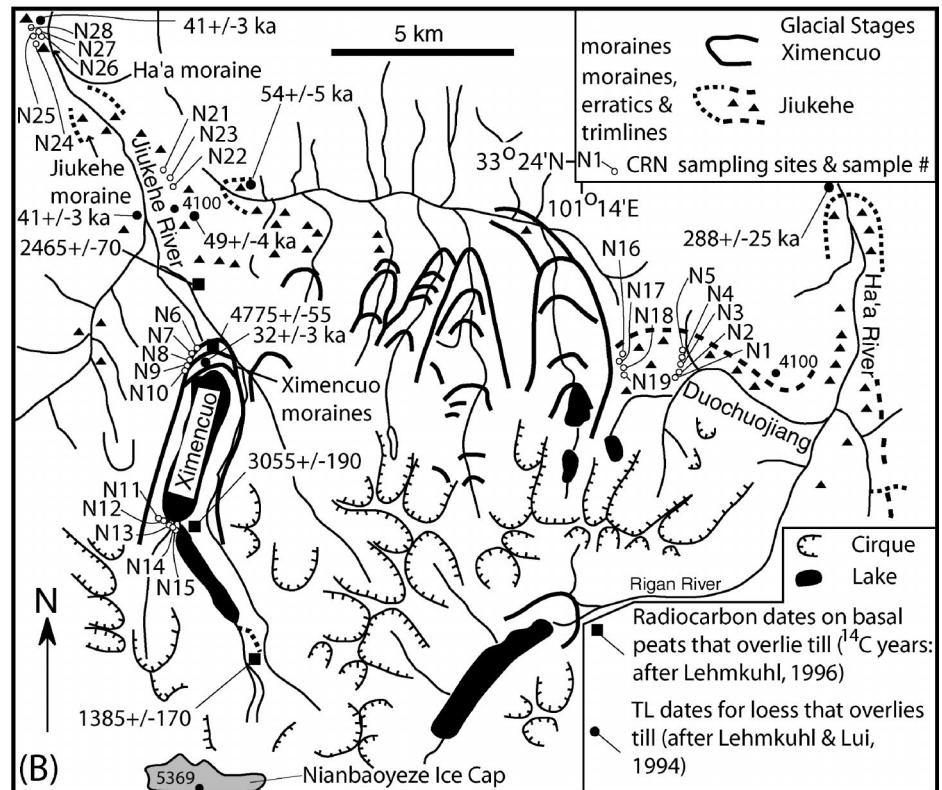
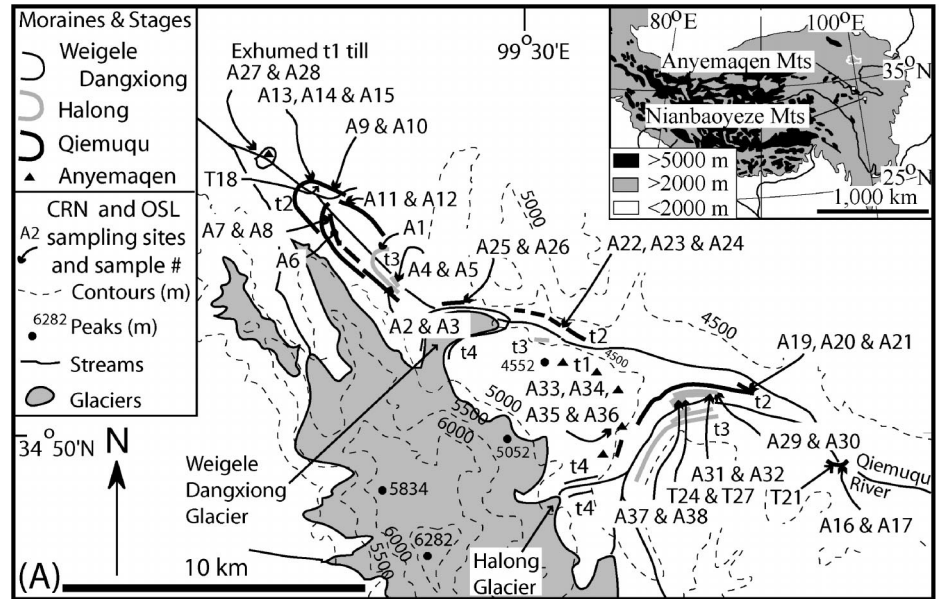


Figure 1. Geomorphic maps of study areas in (A) Anyemaqen Mountains and (B) Nianbaoyeze Mountains. CRN—cosmogenic radionuclides; OSL—optically stimulated luminescence.

decreases from <1000 mm⁻¹ (millimeters per year) to <500 mm⁻¹ from the Nianbaoyeze Mountains northwestward toward the Anyemaqen Mountains (Lehmkuhl and Lui, 1994). Precipitation, however, increases with altitude. In the Anyemaqen Mountains, for example,

precipitation near the snow line (4950–5000 m a.s.l.) is 800 mm⁻¹ and increases to ~1200 mm⁻¹ on the mountain summits (Wang, 1987). The temperature in the region is strongly controlled by altitude, with an environmental lapse rate of ~5.5 °C km⁻¹. The mean an-

nual temperature at 2000 m a.s.l. is $\sim 9.0^\circ\text{C}$ and at ~ 3500 m a.s.l. it is $\sim 1.1^\circ\text{C}$ (Lehmkuhl and Lui, 1994). Snow cover persists in some areas above 4000 m a.s.l. for ~ 10 months of the year, although it is generally thin ($\ll 1$ m thick), and no month is frost-free, leaving the ground frozen for nearly half the year (Lehmkuhl and Lui, 1994). Alpine vegetation, typified by *Saussurea obvallata*, *Saxifrage confertifolia*, and *Aconitum tanguticum*, dominates at altitudes above ~ 4000 m a.s.l. up to the snow line (4800–5100 m a.s.l.) (Lehmkuhl and Lui, 1994).

METHODS

Field Methods and Sampling for Numerical Dating

The glacial geologic evidence was examined along the northern slopes of the Anyemaqen and Nianbaoyeze Mountains using standard geomorphic and sedimentological field techniques. Sites appropriate for CRN dating were identified in both massifs. The sites we selected were concentrated in several valleys in each region where we could clearly identify a succession of morphostratigraphically distinct moraines (Fig. 1). In particular, we focused on the Jiukehe Valley in the Nianbaoyeze Mountains, where Lehmkuhl (1993) and Lehmkuhl and Lui (1994) described type-sites that include the *Ha'a*, *Jiukehe*, and *Ximencuo* moraines (see discussion below).

Rock samples were collected for CRN dating from the surfaces of quartz-rich boulders along moraine crests at locations where there was no apparent evidence of exhumation or slope instability (Fig. 1). Where possible, several boulders were sampled from each moraine ridge to check the reproducibility of the dating and for the possibility of inheritance of CRNs. Photographs and full notes were taken as a record of the degree of weathering and the site conditions for each boulder. The inclination from the boulder site to the top of the surrounding mountain ridges and peaks was measured to determine topographic shielding.

Sampling for OSL dating was undertaken in the Anyemaqen Mountains only. Sediment samples were collected for OSL dating from natural exposures either within or associated with the moraines (Figs. 1 and 2). The OSL samples were obtained by hammering opaque plastic tubes into cleaned, fine-grained sediment sections. If the sediment was too compact to allow successful tube insertion, a block sample was obtained. Once removed, the samples were sealed in plastic and placed in light-

tight sampling bags. Smaller sub-samples were collected to enable replication of water content measurements and for determination of radioisotope concentrations using neutron activation analysis (NAA). All of the samples remained sealed until they were opened in the laboratory. Longitude, latitude, altitude, and depth of overburden were measured, a photographic record was obtained, and detailed graphic sediment logs were constructed (Fig. 2).

CRN Dating

The samples for CRN dating were crushed and sieved. Quartz was separated from the 250–500- μm size fraction using the methods of Kohl and Nishiizumi (1992). After addition of a Be carrier, the Be was separated and purified by ion exchange chromatography and precipitation at $\text{pH} > 7$. The hydroxide was oxidized by ignition in quartz crucibles. BeO was then mixed with Nb metal and loaded into an aluminum target to determine the $^{10}\text{Be}/^{9}\text{Be}$ ratio by accelerator mass spectrometry at the Lawrence Livermore National Laboratory Center for Accelerator Mass Spectrometry (Davis et al., 1990). Isotope ratios were compared to the ICN Pharmaceutical Inc. ^{10}Be standard prepared by K. Nishiizumi (1996, personal commun.) using a half-life of 1.5×10^6 yr.

The measured isotope ratios were converted to radionuclide concentrations in quartz using the total Be in the sample and the sample weights. Radionuclide concentrations were then converted to zero-erosion exposure ages using a sea-level high latitude ^{10}Be production rate of 5.2 at/g-quartz/yr. The Be production rate used is based on a number of independent measurements, as discussed by Owen et al. (2001, 2002a). Production rates were scaled to the latitude and elevation of the sampling sites using the star scaling factors of Lal and Peters (1967) and Lal (1991), as modified by Stone (2000) and a 3% sea-level high latitude muon contribution. Ages were further corrected for changes in the geomagnetic field over time. Details of the calculation are given in Owen et al. (2001, 2002a).

OSL Dating

Quartz grains (90–125 μm or 125–180 μm) were extracted from each sediment sample using standard procedures: sieving, HCl and H_2O_2 treatment, heavy liquid mineral separation with sodium polytungstate, and HF etching. The quartz grains were mounted on stainless steel discs with silicon spray. Luminescence was stimulated with green light (514 Δ 34 nm)

using a Daybreak 1100 OSL system (Bortolot, 1997). Multiple equivalent dose (D_e) values were determined using the single-aliquot regenerative-dose (SAR) protocol (Murray and Wintle, 2000). The distribution in D_e results was assessed using histogram plots. Environmental dose-rates were calculated from radioisotope concentrations and summed together with an estimate for cosmic dose-rate. Further details of preparation and measurement procedures applicable to the samples reported here have been discussed in Owen et al. (2002c, 2003a).

GLACIAL SUCCESSIONS

Wang (1987) provided a map of the glacial landforms in the Anyemaqen Mountains in which he attributed all the landforms to glaciation during the Last Glacial. On the basis of morphostratigraphy and relative weathering, we were able to divide the glacial landforms into four glacial stages that we name the Anyemaqen, Qiemuqu, Halong, and Weigele Dangxiong Glacial Stages (oldest to youngest). Characteristic examples of the moraines for each of these stages are shown in Figure 3.

The Anyemaqen Glacial Stage is represented by subdued and rounded moraine ridges that contain boulders commonly exceeding several meters in diameter. These occur on high surfaces (> 4500 m a.s.l.) above the main valleys and are best seen on the interfluvies between the Weigele Dangxiong and Halong Valleys. Wang (1987) did not map these moraines. The Qiemuqu Glacial Stage is represented by end moraines in the main valleys at altitudes of ~ 4000 m a.s.l. The boulders on these moraines are generally < 1 m in diameter; they are slightly weathered with millimeter-deep pits, and some show slight exfoliation. A series of sharp, crested moraines are present within a few kilometers of the present ice margin and have relatively fresh meter-size boulders on their surfaces. These are assigned to the Halong Glacial Stage. Fresh latero-frontal moraines that enclose the recent glaciers represent the Weigele Dangxiong Glacial Stage.

On the northern slopes of the Nianbaoyeze Mountains, Lehmkuhl (1994) and Lehmkuhl and Lui (1994) recognized evidence for three glaciations. Examples of moraines and glacial deposits in the Nianbaoyeze Mountains are shown in Figure 4. The oldest glaciation in these mountains is represented by the *Ha'a* moraine, which comprises accumulations of meter-size granite erratic boulders distributed

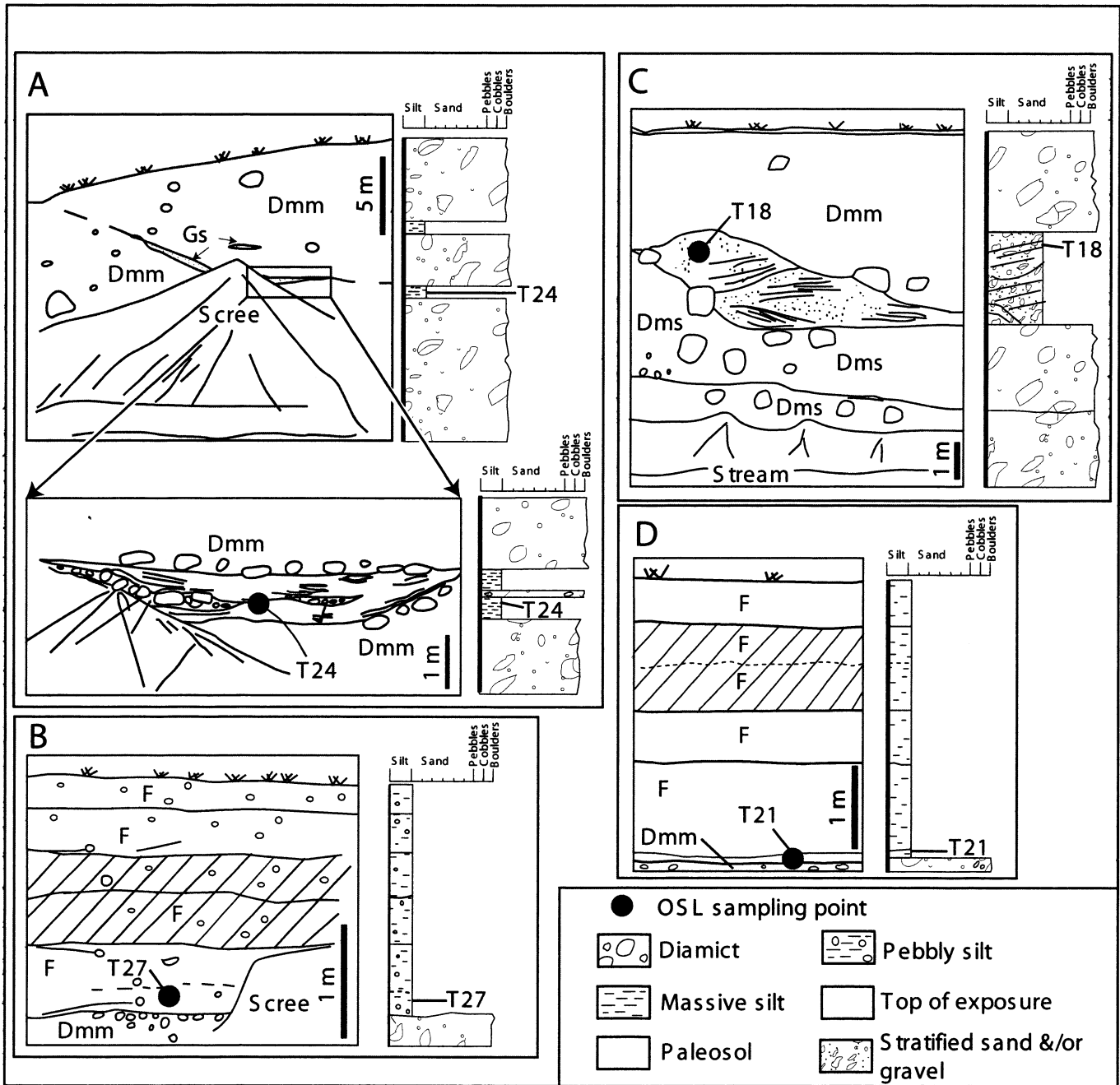


Figure 2. Graphic sedimentary logs showing sampling sites for OSL dating in Anyemaqen Mountains. (A) View looking northward at a stream cutting (at 34°50.365'N/99°32.992'E, 3995 m a.s.l.) within a composite moraine. This landform comprises two till units separated by supraglacial glaciofluvial sediments that were sampled for OSL dating. Upper till was deposited during Halong Glacial Stage; (B) View looking north-northwest at a section within colluviated loess that lies northeast (at 34°50.514'N/99°33.253'E, 4035 m a.s.l.) of section in part A but stratigraphically overlies it; (C) View looking north-northeast in stream cutting through moraine of Qiemuqu Glacial Stage (at 34°54.569'N/99°24.946'E, 4150 m a.s.l.). Samples were collected from within supraglacial channel fills that were subsequently buried beneath supraglacial till; (D) Section in loess that lies immediately above moraine succession shown in part C. Dmm—massive matrix-supported diamict; Dms—stratified matrix-supported diamict; Gs—stratified gravel; F—silt.

along the valley floors and sides (Figs. 1 and 4). This stage has not previously been dated. The next glaciation recognized by Lehmkühl (1994) and Lehmkühl and Lui (1994) is

represented by the Jiukehe moraine, which contains only a few boulders and is covered by 50–70 cm of sandy loess (Figs. 1B and 4). On the basis of the degree of weathering and

erosion of this moraine, as well as by correlation with thermoluminescence (TL)-dated terraces on the Yellow River, Lehmkühl (1994) and Lehmkühl and Lui (1994) ex-

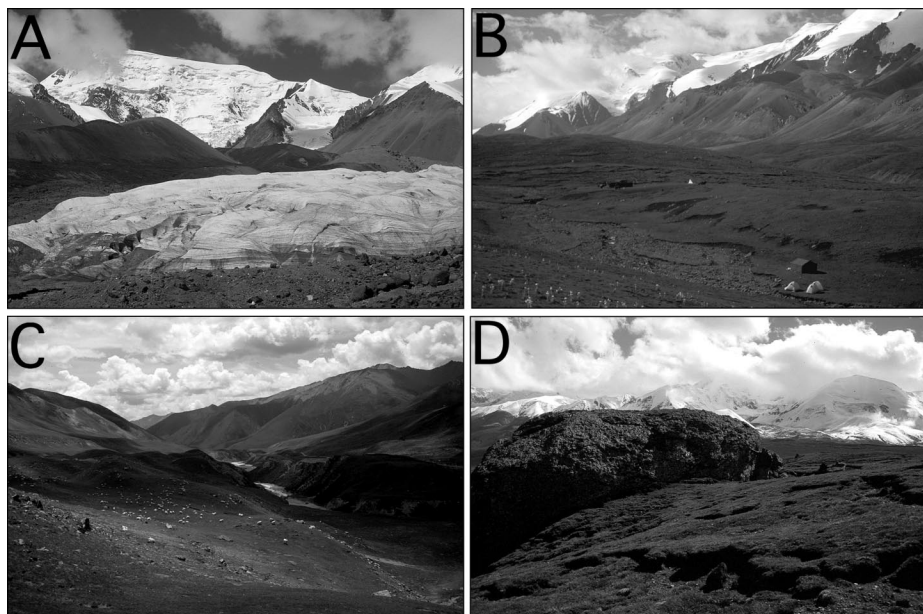


Figure 3. Views of moraines in Anyemaqen Mountains. (A) Looking south at Weigele Dangxiang glacier with moraines of Weigele Dangxiang Glacial Stage adjacent to ice margin (at ~4500 m a.s.l.); (B) A succession of moraines northwest of Weigele Dangxiang Glacier (at ~4250 m a.s.l.) that were formed during Halong Glacial Stage; (C) Looking east-southeast at a latero-frontal moraine complex in Qiemuqu valley (at ~3850 m a.s.l.) that formed during Qiemuqu Glacial Stage; and (D) Erratic northeast section of Halong glacier (at ~4500 m a.s.l.) that was deposited during Anyemaqen Glacial Stage.

pressed the view that this moraine formed >200,000 yr ago.

Lehmkuhl (1994) and Lehmkuhl and Lui (1994) suggested that the Ximencuo moraine provides evidence for the youngest glaciation (Fig. 1B). A 40–60-cm-thick layer of aeolian sandy silt and a 15–20-cm-thick layer of humus cover this moraine through which meter-sized granite boulders protrude (Fig. 1B). On the basis of field mapping, aided by remote sensing, Lehmkuhl (1994) and Lehmkuhl and Lui (1994) correlated moraines around Nianbaoyeze with the Ximencuo moraine and showed that those along the southern slopes of the Nianbaoyeze were at much lower altitudes. They attributed this to greater precipitation that caused glaciers to advance to lower altitudes in the south. They also recognized two younger stages in the Ximencuo Valley, attributing them to the Neoglacial/Late-glacial and the Little Ice Age. On the basis of TL dating of sandy loess capping these moraines, Lehmkuhl (1993) and Lehmkuhl and Lui (1994) suggested that the early stage of this glaciation occurred before 54 ka during MIS-4.

We broadly agree with the mapping and the morphostratigraphic framework presented in Lehmkuhl and Lui (1994). However, our field observations suggest that the Ha'a moraine is not morphostratigraphically distinct from the

Jiukehe moraine. The Jiukehe moraine used to characterize this glaciation by Lehmkuhl and Lui (1994) is probably not a terminal moraine but instead an eroded lateral moraine. Moreover, the Ha'a moraine is an eroded end moraine and may actually represent the terminal position equivalent to the Jiukehe moraine and should be of the same age. To test this difference in interpretation, we collected samples for CRN dating from both the Ha'a and Jiukehe moraines in the Jiukehe Valley.

RESULTS

CRN Dating

The use of surface exposure ages of moraine boulders to determine the timing of glacial advances is open to many sources of uncertainty. Zreda and Phillips (1995) highlighted some of the limitations in determining glacial history by dating moraines using CRN techniques. These problems are further discussed in Owen et al. (2001, 2002a) and Benn and Owen (2002). These studies emphasized that local records may be fragmentary and that deposits of some glacial advances may be incomplete. The record becomes more incomplete the further back in time one goes. Furthermore, moraines may have young apparent

exposure ages due to erosion of moraine surfaces or obliterative overlap and covering of older deposits by younger deposits. Many of these problems can be overcome by undertaking numerous CRN dates on individual moraines and those that are morphostratigraphically similar. Here, we adopt this approach in dating the moraine succession in each of the study areas. The CRN ages determined in this study are listed in Table DR1 and are plotted by moraine and relative age in Figure 5 to show the range and clustering of ages.¹ Such plots allow a qualitative assessment of the potential likelihood that a particular boulder may have a spurious age due to weathering, spalling, exhumation and/or toppling, or due to pre-exposure in another setting. In the discussion below, we have attempted to reject outliers, either younger or older, to obtain a more reliable estimate of the moraine age. The CRN dates in Table DR1 and Figure 5 have not been corrected for weathering. For weathering rates of 1–5 m Ma⁻¹, an exposure age of 10 ka calculated assuming zero erosion would underestimate the true age by 1–4%; an age of 20 ka by 2–9%; and an age of 40 ka by 4–20%.

The oldest moraines in the Anyemaqen Mountains (Anyemaqen Glacial Stage) have CRN ages that range from ca. 20 to 51 ka but cluster around ca. 45 ± 5 ka (omitting A34; $n = 3$) where the error is quoted as one standard deviation. The young age for boulder A34 might be explained by weathering. Given its large size, it is unlikely that boulder A34 has been buried or has toppled. Although we have only sampled a relatively small sample of boulders, we associate the moraines of the Anyemaqen Glacial Stage with MIS-3. This assignment is strengthened by the large number of similar age boulders that were dated for the Jiukehe Glacial Stage in the Nianbaoyeze Mountains, the moraines of which are morphostratigraphically similar to the Anyemaqen Glacial Stage moraines (see results and discussion below).

The next younger set of moraines (Qiemuqu Glacial Stage) in the Anyemaqen Mountains have ages that range from ca. 5 to 28 ka but cluster ca. 16 ± 3 ka (omitting A6, A8, A22, and A24; $n = 16$). Three young outliers A6, A8, and 24 and one old outlier were not included in the average. The moraines of the Qiemuqu Glacial Stage probably formed dur-

¹GSA Data Repository item 2003167, sample numbers, location, and CRN data for boulders on moraines in the Anyemaqen and Nianbaoyeze Mountains, is available on the Web at <http://www.geosociety.org/pubs/ft2003.htm>. Requests may also be sent to editing@geosociety.org.

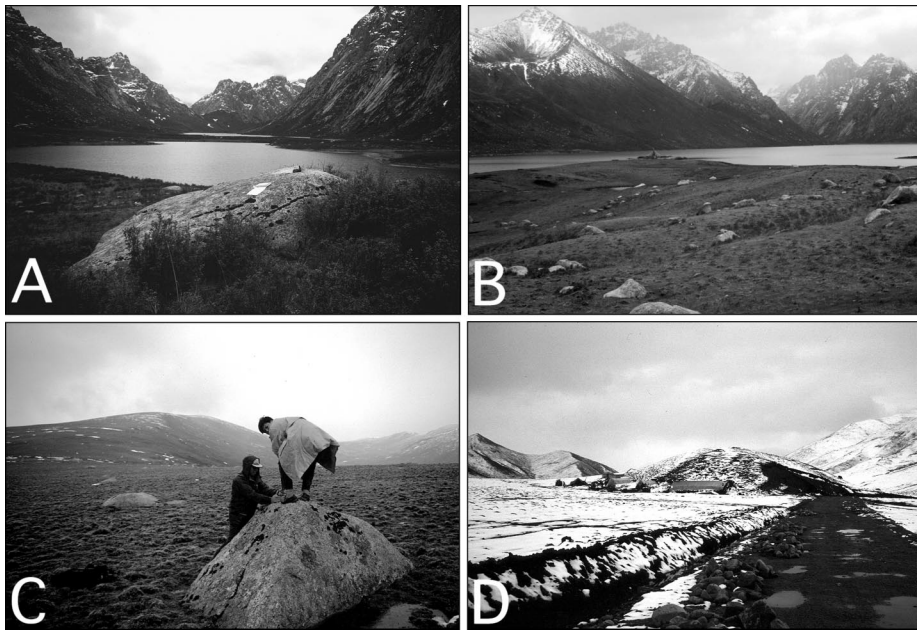


Figure 4. Views of moraines in Nianbaoyeze Mountains. (A) Looking southward across an unnamed lake immediately south of Ximencuo Lake. Boulder in foreground is on crest of a moraine (at ~3950 m a.s.l.) that formed during latter part of Ximencuo Glacial Stage; (B) Looking southward across latero-frontal moraines of Ximencuo Glacial Stage at northern end of Ximencuo Lake (at ~3915 m a.s.l.); (C) Looking northwestward from Duochuojiang River (at ~4150 m a.s.l.) at boulders in moraines of Jiukehe Glacial Stage; and (D) Looking northward at Ha'a moraine (at ~3900 m a.s.l.), which probably formed during Jiukehe Glacial Stage.

ing MIS-2, possibly during the later part of the global Last Glacial Maximum.

The youngest Anyemaqen moraines (Halong Glacial Stage) dated in this study have CRN ages that range from 1 to 12 ka, but cluster ca. 9 ± 3 ka (omitting A3; $n = 10$). One young outlier, A3, was not included in the average. The moraines of the Halong Glacial Stage must have formed during the Early

Holocene. A younger set of moraines is present within a kilometer of the present glaciers, but this was not dated.

On the basis of morphostratigraphy, relative weathering, and the CRN dating, we cannot distinguish between the Ha'a and Jiukehe moraines of Lehmkühl and Lui (1994). We therefore assign these moraines to the Jiukehe Glacial Stage. The CRN dates for this stage vary

from ca. 70 ka to 18 ka. However, the data clusters within MIS-3, with an age of 36 ± 10 ka (omitting as outliers N18, N21, N22, and N26; $n = 14$).

The CRN dates on the Ximencuo moraine (N6-N10) and the younger moraine south of Ximencuo Lake (N13-N15) cluster within MIS-2 at 18 ± 2 ka (omitting N13 and N15; $n = 8$). The old ages on boulders N13 and N15 might be a consequence of inherited CRNs if the boulders were derived from the moraines of the Jiukehe Glacial Stage. We assign the moraines of this age to the Ximencuo Glacial Stage, which is coincident with the global Last Glacial Maximum. However, we might further subdivide this on the basis of morphostratigraphy so that the moraine south of Ximencuo Lake might represent an advance toward the end of the Last Glacial Maximum at 16.5 ± 0.3 ka (omitting N13 and N15; $n = 3$) as compared to the Ximencuo moraine at 20.2 ± 0.7 ka (omitting A9).

OSL Dating

The OSL results are summarized in Table 1. For sample T24 the histogram plot indicated a large spread in the D_e values. Of the 12 D_e measurements made on this sample, 10 values lay between ~90 Gy to 144 Gy and the remaining two D_e results had values of ~240 and 318 Gy. There are several possible reasons for the two higher D_e values, such as inhomogeneous beta microdosimetry, inadequate bleaching of some quartz grains, or environmental mixing of low and high dose grains. However, these two quartz aliquots clearly have anomalously high doses and these results were removed from the data set. The remaining 10 D_e values have a slightly large standard deviation that we consider to be prin-

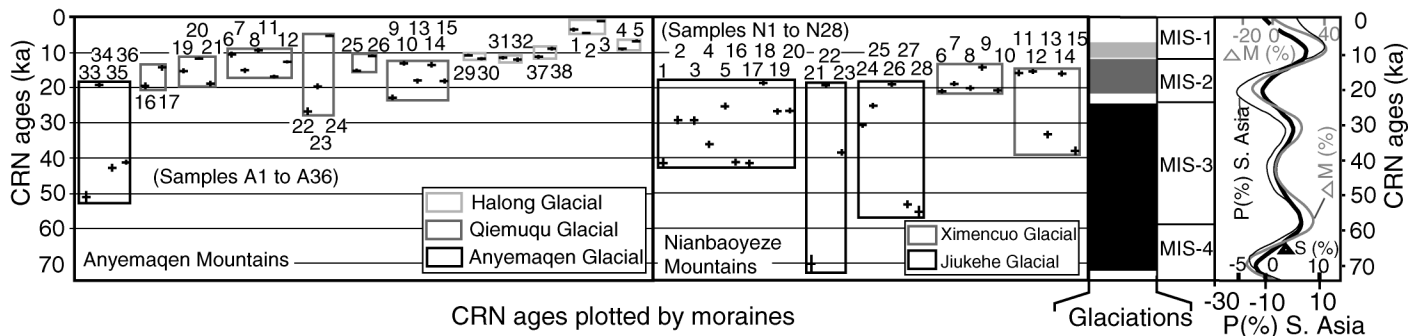


Figure 5. Cosmogenic radionuclide (CRN) ages for moraines in Nianbaoyeze and Anyemaqen Mountains compared with simulated monsoon pressure index (ΔM percentage, solid blue line) for Indian Ocean and simulated changes in precipitation (ΔP percentage, black line) in southern Asia (Prell and Kutzbach, 1987) and variations in Northern Hemisphere solar radiation (ΔS percentage, dashed blue line; Prell and Kutzbach, 1987). Cosmogenic radionuclide ages are plotted along x-axis as per their relative ages. Each box encloses samples from same moraine. Vertical bars for each plotted datum represent analytical error.

TABLE 1. SUMMARY OF OSL DATING RESULTS FROM QUARTZ EXTRACTED FROM SEDIMENT MATRICES: SAMPLE LOCATIONS, RADIOISOTOPE CONCENTRATIONS, MOISTURE CONTENTS, TOTAL DOSE RATE, D_e ESTIMATES, AND OPTICAL AGES

Sample no.	Location (N, E)	a.s.l. (m)	Depth (cm)	U [†] (ppm)	Th [†] (ppm)	K [†] (%)	Rb [†] (ppm)	$W_{in-situ}$ [‡] (%)	Cosmic [§] (mGya ⁻¹)	Dose rate [#] (mGya ⁻¹)	Mean D_e ^{††} (Gy)	Age (ka)
T18	34°54.57', 99°24.95'	4150	300	2.54	11.3	1.71	78.7	1.7	0.244	3.27 ± 0.22	43.17 ± 2.66	13.2 ± 1.2
T21	34°49.35', 99°36.93'	3860	243	2.51	11.5	1.66	81.2	9.4	0.272	3.01 ± 0.19	37.07 ± 2.42	12.3 ± 1.1
T24	34°50.37', 99°32.99'	3995	1000	3.42	17.2	2.05	106.0	11.1	0.092	3.69 ± 0.23	117.69 ± 8.57	31.9 ± 3.1
T27	34°50.51', 99°33.25'	4010	280	2.31	14.4	1.68	93.9	9.5	0.267	3.18 ± 0.20	22.53 ± 1.56	7.1 ± 0.7

[†]Elemental concentrations from NAA of whole sediment. Uncertainty: U ± 0.5 ppm; Th, K, Rb ± 10%.

[‡]Estimated fractional water content from whole sediment (Aitken, 1998). Uncertainty taken as ± 5%.

[§]Estimated contribution to dose rate from cosmic rays (Prescott and Hutton, 1994). Uncertainty taken as ± 10%.

[#]Total dose rate from beta, gamma, and cosmic components. Beta attenuation factors for U, Th, and K compositions calculated using Rainer Grün's "Age" program incorporating grain-size factors from Mejdahl (1979). Beta attenuation factor for Rb arbitrarily taken as 0.75 (cf. Adamiec and Aitken, 1998). Factors utilized to convert elemental concentrations to beta and gamma dose-rates from Adamiec and Aitken (1998) and beta and gamma components attenuated for moisture content.

^{††}Mean D_e . Errors are 1- σ standard errors (ie. $\sigma_{n-1}/n^{1/2}$) incorporating error from beta source ($\pm 5\%$).

cipally due to the expected scatter in interpolation on a saturating exponential growth curve function for samples with high D_e values (cf. Murray et al., 2002). Therefore, the mean of the 10 values was considered to represent the true burial dose. For T18, T21, and T27, the histogram plots showed tight dose distributions, clearly indicating that these samples had all been sufficiently and uniformly bleached; all the D_e values were used to calculate mean D_e results for these samples.

The OSL date for sample T18 (13.2 ± 1.2 ka) provides a depositional age for supraglacial glaciofluvial debris that was subsequently overlain by supraglacial till during the latter part of the Qiemuqu Glacial Stage. This date is consistent with the CRN dates on boulders within this moraine and other moraines that were deposited within the Qiemuqu Glacial Stage. The old age for sample T24 (31.9 ± 3.1 ka) is somewhat problematic. This is because it dates supraglacial glaciofluvial sediments that are interbedded between tills comprising a moraine mapped as being part of the Halong Glacial Stage, which has a CRN surface exposure dated to the Holocene and clearly the OSL date is far older than the CRN dates. The old age might be explained if the moraine were a composite form similar to those described by Richards et al. (2000) and Benn and Owen (2002), resulting from multiple glacial advances. In this case, the lower diamict might represent till deposited during the Anyemaqen stage with the supraglacial glaciofluvial sediments having been deposited during its latter stages. However, this does not explain the absence of till from the Qiemuqu glacial stages.

The OSL dates on loess that stratigraphically overlies these two till sections (samples T21 and T27) provide stratigraphically consistent ages and show that deposition of loess was active during the Late Glacial and Holocene. Both loess sections contain a paleosol (Fig. 2, B and D). This loess postdates T27

(7.1 ± 0.7 ka) and, given its stratigraphic position within the section, it is likely to have formed during the Middle Holocene.

DISCUSSION

Our dating and the morphostratigraphic similarity between the glacial successions in the Anyemaqen and Nianbaoyeze Mountains suggest that glaciations within and between these regions were synchronous during the last 50,000 yr. It is likely that the Anyemaqen and Qiemuqu Glacial Stages, and the Ximencuo and Jiukehe Glacial Stages, respectively, are correlates (Fig. 5).

In both regions, glaciation was most extensive during MIS-3 (Anyemaqen and Jiukehe Glacial Stages), which was represented by expanded ice caps and long valley glaciers that advanced ~15 km beyond the present glacier margins. In the Nianbaoyeze Mountains, Lehmkühl and Lui (1994) present TL dates (41 ± 3 ka, 54 ± 5 ka, and 49 ± 4 ka; Fig. 1B) for loess that overlies landforms formed during the Jiukehe Glacial Stage. These data suggest that the glaciers had retreated from their maximum positions by ca. 50 ka during the Jiukehe Glacial. It is difficult to assess the validity of these TL dates, as no details of the dating methodology, procedures, or analytical results were presented. These dates suggest that the Jiukehe Glacial occurred significantly earlier than is shown by the results presented here, possibly during the early part of MIS-3 or MIS-4. Although there is some evidence from our work of an early MIS-3 advance in the Jiukehe Valley (samples N27 and N28, and on the north slope of the Anyemaqen Mountains, sample A33), significantly more sampling would be required to confirm this. It is intriguing, however, that this early advance would coincide with the $\delta^{18}O$ MIS-3 peak in the Spectral Mapping Project record (Imbrie et al., 1984), while the main advance coincides with the secondary shoulder on the MIS-3

peak. However, the clustering of our CRN dates in both the Nianbaoyeze and Anyemaqen Mountains at ca. 40 ka leads us to believe that the Anyemaqen and Jiukehe Glacial Stages occurred during the early part of MIS-3.

A limited glacial advance during MIS-3/4 supports the view that an ice sheet did not cover the Tibetan Plateau during the Last Glacial (e.g., Li et al., 1991; Derbyshire et al., 1991; Shi et al., 1992; Lehmkühl et al., 1998; Schäfer et al., 2001). Had such an ice sheet developed at that time, the MIS-3 moraines would have been eroded away. Of course, an ice sheet could have existed prior to 50 ka, but there is no evidence of the presence in either of these mountain ranges of moraines older than those we have dated.

Xu and Shen (1995), Zhou et al. (2002), and Yi et al. (2002) have presented evidence for glacier advances during the early part of the last glacial cycle in the Karakunlun Mountains, Qilian Shan, and Puruogangri ice field, respectively. Using TL and electron spin resonance (ESR) dating, they suggest that glaciers advanced during MIS-4 (between ~55–73 ka). However, these dates are poorly defined because they do not directly date the glacial landforms, and the dating cannot be internally checked within each study because only a few dates were obtained. Nevertheless, they support the view that glaciation was more extensive during the earlier part of the last glacial cycle. Our data suggest, however, that glaciation in the Anyemaqen and Nianbaoyeze Mountains occurred during MIS-3 rather than in MIS-4. It is possible that glaciation in the Karakunlun Mountains, Qilian Shan, and Puruogangri ice field was synchronous with the Anyemaqen and Nianbaoyeze Mountains and that the TL and ESR dating needs to be reviewed. Owen et al. (2002b) and Finkel et al. (2003) showed that glaciations were probably synchronous throughout the monsoon-influenced areas of the Himalaya and that glaciers reached their maximum extent during

MIS-3. It is likely that glaciation is also synchronous throughout the monsoonal areas of Tibet and in the Himalaya.

The Qiemuqu and Ximencuo Glacial Stages in the Anyemaqen and Nianbaoyeze Mountains, respectively, date to MIS-2 and were probably broadly coincident with the global Last Glacial Maximum. In both mountain ranges, glaciation during this time was restricted to expanded valley glaciers that extended ≤ 10 km beyond the contemporary glaciers. Similar restricted glacial advances have been dated using CRN and OSL methods to MIS-2 in the La Ji and Qilian Shan Mountains of northern Tibet, and in Litang County in southeastern Tibet (Schäfer et al., 2001; Owen et al., 2003a and b).

In the Anyemaqen, we were able to date a younger glacial stage, the Halong Glacial, to the Early Holocene. This was a valley glaciation that extended only 5–7 km beyond the present glacier margin. We did not find any Early Holocene moraines in our study of the Nianbaoyeze Mountains. Lehmkuhl and Lui (1994), however, mapped moraines only 1–2 km beyond the present ice margin, attributing them to historical advances. It is possible that these moraines are older and might represent an Early Holocene advance, a suggestion that will need to be tested in future studies.

On the basis of multiproxy evidence from ice caps, lake, and pollen records from the Tibetan Plateau, Shi et al. (2001) reconstructed the nature of the Asian monsoon during the later phase of MIS-3, 30–40 ka. They argued that, during this period, lake levels were higher than they are today; alpine steppe-forests shifted ~ 400 km further north, and alpine conifer forests extended ~ 400 – 800 km beyond their present western limits. Furthermore, these authors pointed out that variations in $\delta^{18}\text{O}$ curves from ice cores from the Tibetan Plateau suggest that the temperature was 2–4 °C higher and precipitation 40% to over 100% higher than today. This suggests that the summer monsoon climate over the Plateau from 30 to 40 ka was exceedingly strong, reflecting the 20 ka earth orbital precession cycle; such enhanced solar radiation over the Tibetan plateau region enlarged the thermodynamic contrast between the plateau and the mid-south portion of the Indian Ocean. Such an intensified monsoon and increased precipitation in Tibet would have led to positive glacier mass balances and would help explain the maximum advance of glaciers during MIS-3.

During MIS-2, the lower insolation at this latitude would have reduced the influence of the Asian monsoon. As a consequence, the annual precipitation would have been less and

the mean annual temperature would have been 8–9 °C lower than today (Shi, 2002). These conditions were sufficient to allow glaciers to advance, albeit to a more limited extent than during MIS-3.

The Halong Glacial was coincident with the Early Holocene insolation maximum, suggesting that enhanced monsoon precipitation was also important in forcing glaciation during this time in northeastern Tibet. Similar Holocene advances are recognized throughout the monsoon-influenced areas of the Himalaya (Owen et al., 2002b; Finkel, 2003), further supporting the view that glaciation was synchronous throughout the monsoonal areas of Tibet and the Himalaya.

The findings of our study are therefore in accord with the work of Gillespie and Molnar (1995) and Benn and Owen (1998), indicating that glaciation (i.e., major advances) throughout the Himalaya was asynchronous with the Northern Hemisphere ice sheets. However, the glaciation in these regions during MIS-2 provides evidence that, despite reduced precipitation in northeastern Tibet during the global Last Glacial Maximum, glaciers were still able to advance, albeit to a very limited extent. This pattern and timing of glaciation is similar to the glacial histories of other monsoon-influenced parts of Tibet and the Himalaya and suggests that glaciation was synchronous throughout the monsoon-influenced mountains of high Asia.

CONCLUSIONS

On the basis of morphostratigraphy and numerical dating, new glacial chronologies presented for the Anyemaqen and Nianbaoyeze Mountains suggest that glaciation in these two mountain ranges was synchronous. The maximum extent of glaciation occurred during the early part of the last glacial cycle, in MIS-3. This is the first well-defined succession of moraines dated to MIS-3 in northeastern Tibet. Glaciation during MIS-2 in the global Last Glacial Maximum in these regions was more restricted in extent. An Early Holocene glacial advance is recognized in the Anyemaqen Mountains but is not apparent in the Nianbaoyeze Mountains. The timing of Late Pleistocene and Early Holocene glacial advances in other monsoon-influenced regions of northern Tibet and in the Himalaya is similar, suggesting that glaciation is synchronous throughout the monsoonal regions of high Asia. Furthermore, glacial advances during the insolation maximum support the view that monsoon precipitation is fundamental in controlling the timing and style of glacial advances in this

region. Our chronologies for the Anyemaqen and Nianbaoyeze Mountains should provide a framework to test this climatic link and may provide a tool with which to define rates of surficial geologic processes in the high mountains of Asia.

ACKNOWLEDGMENTS

We thank the National Geographic Society for funding our fieldwork. This work was performed under the auspices of the U.S. Department of Energy by the University of California, Lawrence Livermore National Laboratory (LLNL) under Contract No. W-7405-Eng-48, and as part of an Institute of Geophysics and Planetary Physics (IGPP)/LLNL research grant. We also thank Carrie Patterson, Geoffrey Seltzer, and an anonymous referee for their constructive reviews of our paper.

REFERENCES CITED

- Adamiec, G., and Aitken, M., 1998, Dose-rate conversion factors: update: *Ancient TL*, v. 16, p. 37–50.
- Aitken, M.J., 1998, *An introduction to optical dating*: Oxford, Oxford University Press, 267 p.
- Benn, D.I., and Owen, L.A., 1998, The role of the Indian summer monsoon and the mid-latitude westerlies in Himalayan glaciation: Review and speculative discussion: *Journal of the Geological Society*, v. 155, p. 353–363.
- Benn, D.I., and Owen, L.A., 2002, Himalayan glacial sedimentary environments: A framework for reconstructing and dating former glacial extents in high mountain regions: *Quaternary International*, v. 97–98, p. 3–26.
- Bortolot, V.J., 1997, Improved OSL excitation with fiber-optics and focused lamps: *Radiation Measurements*, v. 27, p. 101–106.
- Bush, A.B.G., 2000, A positive climatic feedback mechanism for Himalayan glaciation: *Quaternary International*, v. 65/66, p. 3–13.
- Bush, A.B.G., 2002, A comparison of simulated monsoon circulations and snow accumulation in Asia during the mid-Holocene and at the Last Glacial Maximum: *Global and Planetary Change*, v. 32, p. 331–347.
- Davis, J.C., Proctor, I.D., Southon, J.R., Caffee, M.W., Heikkinen, D.W., Roberts, M.L., Turteltaub, K.W., Nelson, D.E., Loyd, D.H., and Vogel, J.S., 1990, LLNL/UC AMS facility and research program: *Nuclear Instruments and Methods in Physics Research*, v. B52, p. 269–272.
- Derbyshire, E., Shi, Y., Li, J., Zheng, B., Li, S., and Wang, J., 1991, Quaternary glaciation of Tibet: The geological evidence: *Quaternary Science Reviews*, v. 10, p. 485–510.
- Dey, B., and Bhanu Kumar, O.S.R.U., 1982, An apparent relationship between Eurasian spring snow cover and the advance period of the Indian summer monsoon: *Journal of Applied Meteorology*, v. 21, p. 1929–1923.
- Dey, B., Kathuria, S.N., and Bhanu Kumar, O.S.R.U., 1985, Himalayan snow cover and withdrawal of the Indian summer monsoon: *Journal of Climatology and Applied Meteorology*, v. 24, p. 865–868.
- Dickson, R.R., 1984, Eurasian snow cover versus Indian monsoon rainfall—An extension of the Hahn-Shukla results: *Journal of Climatology and Applied Meteorology*, v. 23, p. 171–173.
- Finkel, R.C., Owen, L.A., Barnard, P.L., and Caffee, M.C., 2003, Beryllium-10 dating of Mount Everest moraines indicates a strong monsoon influence and glacial synchronicity throughout the Himalaya: *Geology*, v. 31, p. 561–564.
- Gillespie, A., and Molnar, P., 1995, Asynchronous maximum advances of mountain and continental glaciers: *Reviews of Geophysics*, v. 33, p. 311–364.
- Hahn, D.G., and Shukla, J., 1976, An apparent relationship between Eurasian snow cover and Indian monsoon

- rainfall: *Journal of Atmospheric Science*, v. 33, p. 2461–2462.
- Kohl, C.P., and Nishiizumi, K., 1992, Chemical isolation of quartz for measurement of in-situ-produced cosmogenic nuclides: *Geochimica et Cosmochimica Acta*, v. 56, p. 3583–3587.
- Imbrie, J., Hays, J.D., Martinson, D.G., McIntyre, A., Mix, A.C., Morley, J.J., Pisias, N.G., Press, W., and Shackleton, N.J., 1984, The orbital theory of Pleistocene climate, in Berger, A.L., ed., Support from a revised chronology of the marine $\delta^{18}\text{O}$ record, in Milankovitch and climate: Boston, D. Reidel, p. 269–305.
- Lal, D., 1991, Cosmic ray labeling of erosion surfaces: In situ nuclide production rates and erosion models: *Earth and Planetary Science Letters*, v. 104, p. 429–439.
- Lal, D., and Peters, B., 1967, Cosmic ray produced radioactivity on the Earth, in Flugge, S., and Sitte, K., eds., *Encyclopedia of Physics, Cosmic Rays II*: Berlin, Springer-Verlag, v. 46, p. 551–612.
- Lehmkuhl, F., 1993, Desertifikation im becken von Zoige (Ruergai Plateau), Osttibet: Berlin, Geogr. Arbeiten, v. 79, p. 82–105.
- Lehmkuhl, F., 1994, Geomorphologische Untersuchungen zum Klima des Holozäns und Jungpleistozäns Osttibets: Habilitationsschrift, Göttingen, 299 p.
- Lehmkuhl, F., and Lui, S., 1994, An outline of physical geography including Pleistocene glacial landforms of eastern Tibet (Provinces Sichuan and Qinghai): *GeoJournal*, v. 34, p. 7–30.
- Lehmkuhl, F., Owen, L.A., and Derbyshire, E., 1998, Late Quaternary glacial history of northeastern Tibet: *Quaternary Proceedings*, v. 6, p. 121–142.
- Li, B., Li, J., and Zhijiu, C., eds., 1991, Quaternary glacier distribution map of Qinghai-Xizang (Tibet) Plateau: Lanzhou, Quaternary Glacier and Environmental Research Center, scale 1:300,000.
- Mejdahl, V., 1979, Thermoluminescence dating: Beta-dose attenuation in quartz grains: *Archaeometry*, v. 21, p. 61–72.
- Molnar, P., and England, P., 1990, Late Cenozoic uplift of mountain ranges and global climatic change: Chicken or egg?, *Nature*, v. 346, p. 29–34.
- Murray, A.S., and Wintle, A.G., 2000, Luminescence dating of quartz using an improved single-aliquot regenerative-dose protocol: *Radiation Measurements*, v. 32, p. 57–73.
- Murray, A.S., Wintle, A.G., and Wallinga, J., 2002, Dose estimation using quartz OSL in the nonlinear region of the growth curve: *Radiation Protection Dosimetry*, v. 101, p. 371–374.
- Owen, L.A., Gualtieri, L., Finkel, R.C., Caffee, M.W., Benn, D.I., and Sharma, M.C., 2001, Cosmogenic radionuclide dating of glacial landforms in the Lahul Himalaya, Northern India: Defining the timing of Late Quaternary glaciation: *Journal of Quaternary Science*, v. 16, p. 555–563.
- Owen, L.A., Finkel, R.C., Caffee, M.W., and Gualtieri, L., 2002a, Timing of multiple glaciations during the Late Quaternary in the Hunza Valley, Karakoram Mountains, Northern Pakistan: Defined by cosmogenic radionuclide dating of moraines: *Geological Society of America Bulletin*, v. 114, p. 593–604.
- Owen, L.A., Finkel, R.C., and Caffee, M.W., 2002b, A note on the extent of glaciation in the Himalaya during the global Last Glacial Maximum: *Quaternary Science Reviews*, v. 21, p. 147–157.
- Owen, L.A., Kamp, U., Spencer, J.Q., and Haserodt, K., 2002c, Timing and style of Late Quaternary glaciation in the eastern Hindu Kush, Chitral, northern Pakistan: A review and revision of the glacial chronology based on new optically stimulated luminescence dating: *Quaternary International*, v. 97–98, p. 41–56.
- Owen, L.A., Teller, J.T., and Rutter, N.W., 2002d, Glaciation and reorganization of Asia's network of drainage: *Global and Planetary Change*, v. 30, p. 289–374.
- Owen, L.A., Spencer, J.Q., Ma, H., Barnard, P.L., Derbyshire, E., Finkel, R.C., Caffee, M.W., and Zeng Yong, N., 2003a, Timing of Late Quaternary glaciation along the southwestern slopes of the Qilian Shan: *Boreas*, v. 32, p. 281–291.
- Owen, L.A., Ma Haizhou, Derbyshire, E., Spencer, J.Q., Barnard, P.L., Zeng Yong Nian, Finkel, R.C., and Caffee, M.W., 2003b, The timing and style of Late Quaternary glaciation in the La Ji Mountains, NE Tibet: Evidence for restricted glaciation during the latter part of the last glacial: *Zeitschrift für Geomorphologie*, v. 130, p. 263–276.
- Prell, W.L., and Kutzbach, J.F., 1987, Monsoon variability over the past 150,000 years: *Journal of Geophysical Research*, v. 92, p. 8411–8425.
- Prell, W.L., and Kutzbach, J.F., 1992, Sensitivity of the Indian monsoon to forcing parameters and implications for its evolution: *Nature*, v. 360, p. 647–652.
- Prescott, J.R., and Hutton, J.T., 1994, Cosmic ray contributions to dose rates for luminescence and ESR dating: Large depths and long-term time variations: *Radiation Measurements*, v. 23, p. 497–500.
- Richards, B.W.M., Benn, D.I., Owen, L.A., Rhodes, E.J., and Spencer, J.Q., 2000a, Timing of Late Quaternary glaciations south of Mount Everest in the Khumbu Himal, Nepal: *Geological Society of America Bulletin*, v. 112, p. 1621–1632.
- Ruddiman, W.F., and Kutzbach, J.E., 1989, Forcing of Late Cenozoic Northern Hemisphere climate by plateau uplift in southern Asia and the America west: *Journal of Geophysical Research*, v. 94, p. 409.
- Schäfer, J.M., Tschudi, S., Zhao, Z., Wu, X., Ivy-Ochs, S., Wieler, R., Baur, H., Kubik, P.W., and Schluchter, C., 2001, The limited influence of glaciations in Tibet on global climate over the past 170,000 yr: *Earth and Planetary Science Letters*, v. 6069, p. 1–11.
- Shi, Y., 2002, Characteristics of Late Quaternary monsoonal glaciation on the Tibetan Plateau and in East Asia: *Quaternary International*, v. 97–98, p. 79–91.
- Shi, Y., Zheng, B., and Li, S., 1992, Last glaciation and maximum glaciation in the Qinghai-Xizang (Tibet) Plateau: A controversy to M. Kuhle's ice sheet hypothesis: *Zeitschrift für Geomorphologie*, v. 84, p. 19–35.
- Shi, Y., Ge, Y., Xiaodong, L., Bingyuan, L., and Tandong, Y., 2001, Reconstruction of the 30–40 ka BP enhanced Indian monsoon climate based on geological records from the Tibetan Plateau: *Palaeogeography, Palaeoclimatology, Palaeoecology*, v. 169, p. 69–83.
- Sirocko, F., Sarnthein, M., Lange, H., and Mayawewski, P.A., 1991, Atmospheric summer circulation and coastal upwelling in the Arabian Sea during the Holocene and the Last Glaciation: *Quaternary Research*, v. 36, p. 72–93.
- Soman, M.K., and Slingo, J., 1997, Sensitivity of the Asian summer monsoon to aspects of sea-surface-temperature anomalies in the tropical Pacific Ocean: *Quarterly Journal of the Royal Meteorological Society*, v. 123, p. 309–336.
- Stone, J.O., 2000, Air pressure and cosmogenic isotope production: *Journal of Geophysical Research*, v. 105, p. 23,753–23,759.
- Wake, C.P., Mayewski, P.A., Dahe, Q., Qinzhao, Y., Sitchang, K., Whitlow, S., and Meeker, L.D., 2001, Changes in atmospheric circulation over the southeastern Tibetan Plateau over the last two centuries from a Himalayan ice core: *PAGES News*, v. 9, p. 14–16.
- Wang, J., 1987, Climatic geomorphology of the northeastern part of the Qinghai-Xizang Plateau, in Hovermann, J., and Wang, W., eds., Reports on the northeastern part of the Qinghai-Xizang (Tibet) Plateau: Beijing, Science Press, p. 140–175.
- Van der Woerd, J., Ryerson, F.J., Tapponnier, P., Meriaux, A.-S., Meyer, B., Gaudemer, Y., Finkel, R.C., Caffee, M.W., Guoguang, Z., and Zhiqin, X., 2002, Uniform post-glacial slip-rate along the central 600 km of the Kunlun Fault (Tibet), from ^{26}Al , ^{10}Be and ^{14}C dating of riser offsets, and climatic origin of the regional morphology: *Geophysical Journal International*, v. 148, p. 356–388.
- Xu, D., and Shen, Y., 1995, On the ice sheet and ice age in the Tibetan Plateau: *Journal of Glaciology and Geocryology*, v. 17, p. 213–229.
- Yi, C., Li, X., and Qu, J., 2002, Quaternary glaciation of Puruogangri—The largest modern ice field in Tibet: *Quaternary International*, v. 97–98, p. 111–123.
- Zhou, S., Li, J., and Zhang, S., 2002, Quaternary glaciation of the Bailang Valley, Qilian Shan: *Quaternary International*, v. 97–98, p. 103–110.
- Zreda, M.G., and Phillips, F.M., 1995, Insights into alpine moraine development from cosmogenic ^{36}Cl buildup dating: *Geomorphology*, v. 14, p. 149–156.

MANUSCRIPT RECEIVED BY THE SOCIETY 27 DECEMBER 2002
 REVISED MANUSCRIPT RECEIVED 12 MAY 2003
 MANUSCRIPT ACCEPTED 21 MAY 2003

Printed in the USA